

**Table III.** Bond Angles (deg) and Their Estimated Standard Deviations

OW-K1-OW	146.57 (7)	K1-O1-H3	109 (2)
OW-K1-O1	69.97 (4)	B1-O1-H3	109 (2)
OW-K1-O1	121.54 (5)	K2-O2-B1	127.1 (1)
OW-K1-O4	116.45 (4)	K2-O2-H4	105 (2)
OW-K1-O4	87.59 (4)	B1-O2-H4	111 (2)
OW-K1-O6	80.52 (4)	B1-O3-B3	124.2 (2)
OW-K1-O6	73.55 (4)	K1-O4-B1	94.6 (1)
O1-K1-O1	143.39 (6)	K1-O4-B2	117.0 (1)
O1-K1-O4	48.60 (4)	B1-O4-B2	123.5 (2)
O1-K1-O4	102.76 (4)	K2-O5-B2	138.1 (1)
O1-K1-O6	75.60 (4)	K2-O5-H5	98 (3)
O1-K1-O6	137.55 (4)	B2-O5-H5	115 (3)
O1-K1-O4	102.76 (4)	K1-O6-B2	118.3 (1)
O4-K1-O4	90.95 (5)	K1-O6-B3	119.1 (1)
O4-K1-O6	96.58 (4)	B2-O6-B3	118.8 (2)
O4-K1-O6	167.85 (4)	K2-O7-B3	113.2 (1)
O6-K1-O6	77.71 (5)	K2-O7-H6	93 (2)
O2-K2-O2	180.00	B3-O7-H6	117 (3)
O2-K2-O5	74.33 (5)	O1-B1-O2	110.1 (2)
O2-K2-O5	105.67 (5)	O1-B1-O3	109.3 (2)
O2-K2-O7	76.17 (4)	O1-B1-O4	108.7 (2)
O2-K2-O7	103.83 (4)	O2-B1-O3	108.1 (2)
O5-K2-O5	180.00	O2-B1-O4	110.2 (2)
O5-K2-O7	90.03 (5)	O3-B1-O4	110.5 (2)
O5-K2-O7	89.97 (5)	O4-B2-O5	118.6 (2)
O7-K2-O7	180.00	O4-B2-O6	121.5 (2)
K1-OW-H1	121 (2)	O5-B2-O6	119.9 (2)
K1-OW-H2	103 (2)	O3-B3-O6	121.2 (2)
H1-OW-H2	105 (3)	O3-B3-O7	118.1 (2)
K1-O1-B1	106.8 (1)	O6-B3-O7	120.7 (2)

The final coefficient, refined by least squares, was 0.0000007 (in absolute units).

The structure was solved by using direct methods. Hydrogen atoms were located and their positions and isotropic thermal parameters were refined. The structure was refined by full-matrix least squares where the function minimized was  $\sum w(|F_o| - |F_c|)^2$  and the weight  $w$  is defined as  $4F_o^2/\sigma^2(F_o^2)$ . The standard deviation on intensities,  $\sigma(F_o^2)$ , is defined as follows:

$$\sigma^2(F_o^2) = [S^2(C + R^2B) + (pF_o^2)^2]/L^2$$

where  $S$  is the scan rate,  $C$  is the total integrated peak count,  $R$  is the

ratio of scan time to background counting time,  $B$  is the total background count,  $L$  is the Lorentz-polarization factor, and the parameter  $p$  is a factor introduced to downweight intense reflections. Here  $p$  was set to 0.050. Scattering factors were those tabulated by Cromer and Waber.<sup>26</sup> Anomalous dispersion effects were included in  $F_c$ ;<sup>27</sup> the values for  $\Delta f'$  and  $\Delta f''$  were those of Cromer.<sup>28</sup> Only the 1165 reflections having intensities greater than 3.0 times their standard deviation were used in the refinements. The final cycle of refinement included 136 variable parameters and converged (largest parameter shift was 0.06 times its esd) with unweighted and weighted agreement factors of

$$R_1 = \sum ||F_o| - |F_c|| / \sum |F_o| = 0.029$$

$$R_2 = [\sum w(|F_o| - |F_c|)^2 / \sum wF_o^2]^{1/2} = 0.041$$

The standard deviation of an observation of unit weight was 1.22. The highest peak in the final difference Fourier had a height of  $0.28 \text{ e}/\text{\AA}^3$  with an estimated error based on  $\Delta F^{29}$  of 0.07. Plots of  $\sum w(|F_c| - |F_o|)^2$  vs.  $|F_o|$ , reflection order in data collection,  $(\sin \theta)/\lambda$ , and various classes of indices showed no unusual trends. The computer was a PDP-11/60-based system. Positional parameters are listed in Table I. Bond distances and angles are collected in Tables II and III. Tables of observed and calculated structure factor amplitudes, thermal parameters, least-squares planes, and intermolecular contacts are available as supplementary material. The calculated X-ray powder pattern for Cu radiation is also available.

**Acknowledgment.** We thank O. L. Davis for the many powder diffraction spectra and assistance with the oven experiments and Dr. R. C. Medrud for preliminary crystal analysis and the calculated X-ray powder pattern.

**Supplementary Material Available:** Tables of anisotropic thermal parameters, weighted least-squares planes, and intermolecular contacts to 3.50 Å for I, the 40 most intense lines in the calculated X-ray powder pattern of I for Cu radiation, and complete X-ray powder patterns for  $\beta$ -KB<sub>3</sub>O<sub>5</sub> and  $\gamma$ -KB<sub>3</sub>O<sub>5</sub> and a stereoview of the unit cell of I (9 pages); a table of observed and calculated structure factors for I (4 pages). Ordering information is given on any current masthead page.

- (26) Cromer, D. T.; Waber, J. T. In *International Tables for X-ray Crystallography*; Kynoch: Birmingham, England, 1974; Vol. IV, Table 2.2B.  
 (27) Ibers, J. A.; Hamilton, W. C. *Acta Crystallogr.* **1964**, *17*, 781.  
 (28) Cromer, D. T. In *International Tables for X-ray Crystallography*; Kynoch: Birmingham, England, 1974; Vol. IV, Table 2.3.1.  
 (29) Cruickshank, D. W. J. *Acta Crystallogr.* **1949**, *2*, 154.

Contribution from the Departments of Chemistry, Colorado State University, Fort Collins, Colorado 80523, University of Colorado at Denver, Denver, Colorado 80202, and University of Denver, Denver, Colorado 80208

## Metal-Nitroxyl Interactions. 49. Molecular Structure and EPR Spectra of Dichloro(bis((1-pyrazolyl)methyl)(2,2,6,6-tetramethyl-1-oxy-4-piperidinyl)amine)copper(II) and EPR Studies of Copper-Nitroxyl Exchange in Related Compounds

Joseph H. Reibenspies,<sup>1a</sup> Oren P. Anderson,\*<sup>1a</sup> Sandra S. Eaton,\*<sup>1b</sup> Kundalika M. More,<sup>1c</sup> and Gareth R. Eaton\*<sup>1c</sup>

Received July 17, 1986

The structure of the title compound, Cu(bp-NO)Cl<sub>2</sub>, has been investigated by single-crystal X-ray diffraction. Discrete molecules of Cu(bp-NO)Cl<sub>2</sub> crystallize in the monoclinic space group  $P2_1/c$  ( $Z = 4$ ), with  $a = 11.737$  (4) Å,  $b = 11.744$  (4) Å,  $c = 15.326$  (4) Å, and  $\beta = 94.03$  (2)°. In Cu(bp-NO)Cl<sub>2</sub>, the three nitrogen atoms of the bp-NO ligand and two chloride ions surround the copper(II) ion in a distorted square pyramidal array. One of the chloride ions occupies the more weakly bound apical position (Cu-Cl1 = 2.495 (1) Å), while the second occupies a basal position (Cu-Cl2 = 2.231 (1) Å). The Cu-N(amine) bond distance (2.195 (3) Å) is much longer than the Cu-N(pyrazole) bond distances (1.965 (3), 1.957 (4) Å). The magnitude of the copper-nitroxyl exchange coupling constant,  $J$ , in a series of copper(II) complexes of spin-labeled bis(pyrazolyl)amines ranged from >3500 to <100 G. It is proposed that the magnitude of  $J$  reflects the strength of the bond between the copper(II) and the amine nitrogen that is attached to the spin label.

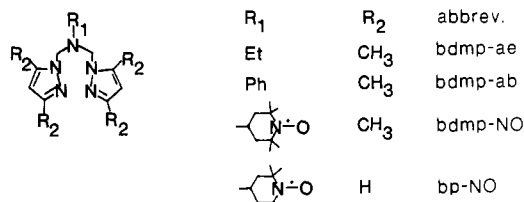
### Introduction

Recently, it has been shown that reaction of 1-(hydroxymethyl)-3,5-dimethylpyrazole with primary amines (RNH<sub>2</sub>)

produces the bis(pyrazolyl)amine bdmp-R.<sup>2</sup> The structures of four transition-metal complexes of these ligands have been determined. In Ni(bdmp-ae)(NO<sub>3</sub>)<sub>2</sub>, the metal was in a distorted octahedral environment and the distance between the Ni(II) atom

(1) (a) Colorado State University. (b) University of Colorado at Denver. (c) University of Denver.

(2) Driessen, W. L. *Recl. Trav. Chim. Pays-Bas* **1982**, *101*, 441.



and the amine nitrogen atom was 2.128 (5) Å.<sup>3</sup> In Cu(bp-ae)Br<sub>2</sub>, the metal was in a distorted square pyramidal environment and the distance between the copper(II) atom and the amine nitrogen atom was 2.191 (2) Å.<sup>4</sup> In Cu(bdmp-ab)Br<sub>2</sub>, the metal was in a distorted trigonal bipyramidal environment and the distance between the Cu(II) atom and the amine nitrogen atom was 2.423 (1) Å.<sup>5</sup> In Co(bdmp-ab)Cl<sub>2</sub> the metal was in a distorted tetrahedral environment and the amine nitrogen atom was not coordinated.<sup>5</sup> These structures indicate that bis(pyrazolyl)amines can function as flexible bidentate or tridentate ligands and that there can be considerable variation in the length of the bond to the amine nitrogen. This raises the possibility that the bonding between Cu(II) and the amine nitrogen atom in a bis(pyrazolyl)amine complex might be sensitive to changes in the pyrazole substituents and in the anion.

The electron-electron spin-spin interaction between a paramagnetic transition metal and a nitroxyl radical is a sensitive probe of the bonding pathway between the two paramagnetic centers. It therefore appeared likely that it would be possible to use copper-nitroxyl interactions to study the binding of the amine nitrogen atom in copper complexes of a spin-labeled bis(pyrazolyl)amine. We have prepared the spin-labeled ligands bdmp-NO and bp-NO and the corresponding copper(II) complexes. EPR spectra of Cu(bp-NO)X<sub>2</sub> (X = Cl, Br) and Cu(bdmp-NO)X<sub>2</sub> (X = Cl, Br, ClO<sub>4</sub>, BF<sub>4</sub>) were examined. Structure determination was carried out by single-crystal X-ray diffraction.

## Experimental Section

**Physical Measurements.** Visible spectra were obtained in dichloromethane or toluene solutions on a Cary 14 spectrometer with the OLIS modification.<sup>6</sup> Visible spectra are given below with band maxima in nanometers and log  $\epsilon$  in parentheses. Infrared spectra were obtained in Nujol mulls or KBr pellets on a Perkin-Elmer 283B spectrometer. Melting points were obtained on a Hoover Mel-Temp apparatus. Mass spectra were obtained by fast atom bombardment (FAB) of samples in a glycerol matrix. Under these conditions the Cu(II) was reduced to Cu(I). X-Band EPR spectra were obtained with 100-kHz modulation on a Varian E9 interfaced to an IBM CS9000 or on an IBM ER200D interfaced to an IBM CS9000. Q-Band spectra were obtained on a spectrometer that has been described previously.<sup>7</sup> Solutions were about  $1 \times 10^{-3}$  M. The lines in the spectra were sufficiently broad that the spectra were not changed by degassing the samples. Spectra were obtained with microwave powers that did not cause saturation and modulation amplitudes that did not distort the line shapes.

**Preparation of Ligands.** Bis((3,5-dimethyl-1-pyrazolyl)methyl)phenylamine, bdmp-ab, was prepared as reported in the literature.<sup>2,5</sup>

**Bis((3,5-dimethyl-1-pyrazolyl)methyl)(2,2,6,6-tetramethyl-1-oxy-4-piperidinyl)amine, bdmp-NO.** The spin-labeled ligand was prepared by a procedure similar to that reported for bdmp-ab.<sup>2,5</sup> 1-(Hydroxymethyl)-3,5-dimethylpyrazole<sup>2</sup> (1.26 g, 10 mmol) was added to a solution of 4-amino-2,2,6,6-tetramethylpiperidinyl-1-oxy (0.856 g, 5.0 mmol) in 1,2-dichloroethane (10 mL). The solution was stirred for 24 h. The dichloroethane layer was separated from the water layer, and the dichloroethane was removed under vacuum. The resulting red solid was

recrystallized from hexane: yield 1.84 g, 95%; mp 60 °C. IR: 1560, 1465, 1380, 1320, 1240, 1200, 1100, 1030, 980, 780, 720 cm<sup>-1</sup>.

**Bis((1-pyrazolyl)methyl)(2,2,6,6-tetramethyl-1-oxy-4-piperidinyl)amine, bp-NO.** The ligand was prepared from 1-(hydroxymethyl)pyrazole and 4-amino-2,2,6,6-tetramethylpiperidinyl-1-oxy by a procedure similar to that reported for bdmp-NO: yield 80%; mp 105 °C. IR: 1450, 1380, 1240, 1180, 1130, 1085, 960, 750, 615 cm<sup>-1</sup>.

**Preparation of Copper Complexes.** Cu(bdmp-ab)Cl<sub>2</sub> was prepared as previously reported;<sup>5</sup> mp 139 °C (lit.<sup>5</sup> mp 140–141 °C). IR: 1600, 1555, 1465, 1415, 1385, 1315, 1280, 1210, 1180, 1125, 1060, 975, 810, 800, 770, 755, 690, 615 cm<sup>-1</sup>. Vis (dichloromethane): 850 (2.36), 374 (3.13), 281 (3.64) nm. Mass spectrum: (M - 2Cl)<sup>+</sup>, m/z = 442 for <sup>63</sup>Cu.

**Dichloro(bis((3,5-dimethyl-1-pyrazolyl)methyl)(2,2,6,6-tetramethyl-1-oxy-4-piperidinyl)amine)copper(II), Cu(bdmp-NO)Cl<sub>2</sub>.** The complex was prepared by a procedure analogous to that reported for Cu(bdmp-ab)Cl<sub>2</sub>.<sup>5</sup> CuCl<sub>2</sub>·2H<sub>2</sub>O (0.17 g, 1.0 mmol) was dissolved in absolute ethanol (5 mL) and treated with triethyl orthoformate (1 mL) to remove water. A solution of bdmp-NO (0.388 g, 1.0 mmol) in absolute ethanol (2 mL) was added. A green solid crystallized from the solution at room temperature within 10 min of mixing the reactants. The crystals were collected by filtration, washed with about 1 mL of absolute ethanol, and then washed several times with dry diethyl ether; yield 0.40 g, 77%. Prolonged heating under vacuum caused decomposition; mp 179 °C. IR: 1460, 1400, 1305, 1270, 1240, 1200, 1180, 1120, 1060, 975, 880, 790, 670, 610 cm<sup>-1</sup>. Vis (dichloromethane): 895 (2.41), 365 (3.13) nm. Vis (1:1 dichloromethane-toluene): 900 (2.43), 360 (3.21) nm.

**Dichloro(bis((1-pyrazolyl)methyl)(2,2,6,6-tetramethyl-1-oxy-4-piperidinyl)amine)copper(II), Cu(bp-NO)Cl<sub>2</sub>.** This complex was prepared from bp-NO and CuCl<sub>2</sub>·2H<sub>2</sub>O by a procedure similar to that used to prepare Cu(bdmp-NO)Cl<sub>2</sub>: yield 82%; mp 168 °C. IR: 1450, 1400, 1375, 1320, 1270, 1240, 1200, 1185, 1130, 1090, 1060, 980, 870, 825, 790, 755, 680, 600 cm<sup>-1</sup>. Mass spectrum: (M - 2Cl)<sup>+</sup>, m/z = 395 for <sup>63</sup>Cu. Crystals used in the X-ray diffraction study were grown from absolute ethanol.

**Dibromo(bis((3,5-dimethyl-1-pyrazolyl)methyl)(2,2,6,6-tetramethyl-1-oxy-4-piperidinyl)amine)copper(II), Cu(bdmp-NO)Br<sub>2</sub>.** This complex was prepared from bdmp-NO and CuBr<sub>2</sub> by a procedure similar to that used to prepare Cu(bdmp-NO)Cl<sub>2</sub>: yield 75%; mp 158 °C. IR: 1460, 1400, 1300, 1275, 1240, 1200, 1180, 1120, 1060, 970, 880, 790, 670, 600 cm<sup>-1</sup>. Vis (dichloromethane): 900 (2.80), 418 (3.31), 309 (3.80) nm. Vis (1:1 toluene-dichloromethane): 900 (2.70), 424 (3.35), 310 (3.50) nm. Vis (toluene, saturated): 895, 424, 310 nm.

**Dibromo(bis((1-pyrazolyl)methyl)(2,2,6,6-tetramethyl-1-oxy-4-piperidinyl)amine)copper(II), Cu(bp-NO)Br<sub>2</sub>.** This complex was prepared from bp-NO and CuBr<sub>2</sub> by a procedure similar to that used to prepare Cu(bdmp-NO)Cl<sub>2</sub>: yield 80%; mp 185 °C. IR: 1460, 1400, 1380, 1320, 1270, 1240, 1200, 1185, 1130, 1090, 1065, 985, 875, 830, 780, 755, 680 cm<sup>-1</sup>. Vis (dichloromethane): 900 (2.18), 420 (2.60), 338 (2.94) nm.

**Bis(perchlorato)(bis((3,5-dimethyl-1-pyrazolyl)methyl)(2,2,6,6-tetramethyl-1-oxy-4-piperidinyl)amine)copper(II), Cu(bdmp-NO)(ClO<sub>4</sub>)<sub>2</sub>.** The complex was prepared from Cu(ClO<sub>4</sub>)<sub>2</sub> and bdmp-NO by a procedure similar to that used to prepare Cu(bdmp-NO)Cl<sub>2</sub>. Since the complex did not precipitate from the reaction mixture, the solvent was removed and the residue was washed with dry diethyl ether to give a green solid: yield 78%; mp 120 °C dec. IR: 1550, 1465, 1380, 1240, 1100 (vs, multiple peaks), 800, 600 cm<sup>-1</sup>. Vis (dichloromethane, saturated): 610, 360 nm.

**Bis(perchlorato)(bis((3,5-dimethyl-1-pyrazolyl)methyl)phenylamine)copper(II), Cu(bdmp-ab)(ClO<sub>4</sub>)<sub>2</sub>.** The complex was prepared from Cu(ClO<sub>4</sub>)<sub>2</sub> and bdmp-ab by the procedure used to prepare Cu(bdmp-NO)(ClO<sub>4</sub>)<sub>2</sub>: yield 65%; mp 136 °C dec. IR: 1600, 1580, 1550, 1490, 1420, 1390, 1100 (vs, multiple peaks), 925, 800, 700, 625 cm<sup>-1</sup>. Vis (dichloromethane, saturated): 616, 378 nm.

**Bis(tetrafluoroborato)(bis((3,5-dimethyl-1-pyrazolyl)methyl)(2,2,6,6-tetramethyl-1-oxy-4-piperidinyl)amine)copper(II), Cu(bdmp-NO)(BF<sub>4</sub>)<sub>2</sub>.** The complex was prepared from bdmp-NO and Cu(BF<sub>4</sub>)<sub>2</sub> by the procedure used to prepare Cu(bdmp-NO)(ClO<sub>4</sub>)<sub>2</sub>: yield 70%; mp 117 °C dec. IR: 1550, 1460, 1390, 1300, 1240, 1120 (s), 1080 (s), 1040 (s), 790, 690, 530, 520 cm<sup>-1</sup>. Vis (dichloromethane, saturated): 602 nm.

**Structure Determination for Cu(bp-NO)Cl<sub>2</sub>.** Crystal data for Cu(bp-NO)Cl<sub>2</sub>, together with details of the X-ray diffraction experiment and subsequent computations, are listed in Table I. Cell dimensions were obtained from a least-squares fit to the setting angles for 25 reflections ( $2\theta_{av} = 17.04^\circ$ ) on a Nicolet R3m diffractometer.<sup>8</sup> The stability of the

(3) Schoonhoven, J. W. F. M.; Driessen, W. L.; Reedijk, J.; Verschoor, G. C. *J. Chem. Soc., Dalton Trans.* **1984**, 1053.

(4) Veldhuis, J. B. J.; Driessen, W. L.; Reedijk, J. *J. Chem. Soc., Dalton Trans.* **1986**, 537.

(5) Blonk, H. L.; Driessen, W. L.; Reedijk, J. *J. Chem. Soc., Dalton Trans.* **1985**, 1699.

(6) The On-Line Instruments System (OLIS) 3920 modification replaces the Cary 14 electronics with stepper motors for the slit and monochromator and controls the system with a Zenith Z-100 microcomputer with 13-bit A/D and D/A converters.

(7) Eaton, S. S.; More, K. M.; DuBois, D. L.; Boymel, P. M.; Eaton, G. R. *J. Magn. Reson.* **1980**, *41*, 150.

(8) Software used for diffractometer operations and data collection was provided with the Nicolet R3m diffractometer. Crystallographic computations were carried out with the SHELXTL program library, written by G. M. Sheldrick and supplied by Nicolet XRD for the Data General Eclipse S/140 computer in the crystallography laboratory at Colorado State University.

**Table I.** Details of the Crystallographic Experiment and Computations for [Cu(bp-NO)Cl<sub>2</sub>]

formula	C <sub>17</sub> H <sub>27</sub> N <sub>6</sub> Cl <sub>2</sub> CuO
fw	465.9
cryst syst	monoclinic
space group	<i>P</i> <sub>2</sub> <sub>1</sub> / <i>c</i>
<i>a</i> , Å	11.737 (4)
<i>b</i> , Å	11.744 (4)
<i>c</i> , Å	15.326 (4)
$\beta$ , deg	94.03 (2)
<i>V</i> , Å <sup>3</sup>	2107
temp, °C	-125 °C
<i>Z</i>	4
<i>F</i> (000)	968
$\rho$ (calcd), g cm <sup>-3</sup>	1.47
cryst dims, mm	0.04 (100 → $\bar{1}$ 00) × 0.22 (010 → 0 $\bar{1}$ 0) × 0.36 (001 → 00 $\bar{1}$ )
radiation	Mo K $\alpha$ ( $\lambda$ = 0.7107 Å)
monochromator	graphite
$\mu$ , cm <sup>-1</sup>	13.2
scan type	$\theta/2\theta$
geometry	bisecting
$2\theta$ range, deg	4.0–50.0
scan speed, deg min <sup>-1</sup>	variable, 2.02–29.30
index restrictions	-14 ≤ <i>h</i> ≤ 14, 0 ≤ <i>k</i> ≤ 14, -19 ≤ <i>l</i> ≤ 0
reflens	4229 measd, 4067 unique, 3005 used ( $ F_o  > 2.5\sigma( F_o )$ )
no. of least-squares params	256
data/params	11.7
<i>R</i>	0.053
<i>R</i> <sub>w</sub>	0.048
GOF	1.24
<i>g</i>	6.3 × 10 <sup>-4</sup> (refined)
slope, norm prob plot	1.12

**Table II.** Fractional Atomic Coordinates (×10<sup>4</sup>) and Isotropic Thermal Parameters (Å<sup>2</sup> × 10<sup>3</sup>) for [Cu(bp-NO)Cl<sub>2</sub>]<sup>a</sup>

atom	<i>x</i>	<i>y</i>	<i>z</i>	<i>U</i> <sub>iso</sub> <sup>b</sup>
Cu	1444 (1)	6562 (1)	1914 (1)	20 (1)
Cl1	-381 (1)	6954 (1)	1031 (1)	23 (1)
Cl2	2397 (1)	8138 (1)	2327 (1)	34 (1)
N1	629 (3)	6350 (3)	2979 (2)	19 (1)
N2	57 (3)	5345 (3)	2999 (2)	19 (1)
C1	496 (4)	6852 (4)	3741 (3)	26 (1)
C2	-184 (4)	6189 (4)	4245 (3)	30 (2)
C3	-443 (4)	5222 (4)	3755 (3)	24 (1)
N3	2318 (3)	6187 (3)	912 (2)	23 (1)
N4	2055 (3)	5127 (3)	579 (2)	23 (1)
C4	3173 (4)	6552 (4)	486 (3)	37 (2)
C5	3473 (5)	5754 (5)	-130 (4)	54 (2)
C6	2750 (4)	4850 (4)	-47 (3)	36 (2)
C7	143 (3)	4515 (3)	2292 (3)	20 (1)
C8	1131 (4)	4513 (4)	945 (3)	23 (1)
N5	1224 (3)	4706 (3)	1896 (2)	17 (1)
C9	2258 (3)	4136 (3)	2345 (2)	16 (1)
C10	2294 (3)	2853 (3)	2199 (3)	20 (1)
C11	3385 (4)	2289 (4)	2608 (3)	23 (1)
N6	3606 (3)	2681 (3)	3523 (2)	21 (1)
C12	3424 (4)	3874 (4)	3803 (3)	22 (1)
C13	2340 (3)	4356 (3)	3322 (3)	19 (1)
C14	3234 (4)	3844 (4)	4782 (3)	33 (2)
C15	4480 (4)	4604 (4)	3652 (3)	33 (2)
C16	3212 (4)	1005 (4)	2623 (3)	31 (2)
C17	4429 (4)	2573 (4)	2090 (3)	30 (2)
O	4317 (3)	2091 (3)	4016 (2)	35 (1)

<sup>a</sup>Estimated standard deviations in the least significant digits are given in parentheses. <sup>b</sup>*U*<sub>iso</sub> is defined as one-third of the trace of the *U*<sub>ij</sub> tensor.

crystal in the X-ray beam was monitored by measurement of the intensities of 3 control reflections (204, 121, 211) every 97 reflections. No significant change in the intensities of these 3 reflections was noted. An empirical absorption correction was performed, utilizing the intensity profiles obtained for 10 reflections as a function of  $\psi$  ( $\Delta\psi = 15^\circ$ ). The range of transmission factors exhibited for the complete data set was 0.426–0.489. The merging *R* decreased from 0.029 before the correction to 0.0242 after correction. In addition to the absorption correction,

**Table III.** Bond Lengths (Å) and Angles (deg) for [Cu(bp-NO)Cl<sub>2</sub>]<sup>a</sup>

a. Bond Lengths			
Cu–Cl1	2.495 (1)	Cu–Cl2	2.231 (1)
Cu–N1	1.965 (3)	Cu–N3	1.957 (4)
Cu–N5	2.195 (3)	N1–N2	1.360 (5)
N1–C1	1.327 (5)	N2–C3	1.342 (5)
N2–C7	1.466 (5)	C1–C2	1.388 (6)
C2–C3	1.384 (6)	N3–N4	1.372 (5)
N3–C4	1.307 (6)	N4–C6	1.343 (6)
N4–C8	1.448 (5)	C4–C5	1.392 (8)
C5–C6	1.372 (8)	C7–N5	1.461 (5)
C8–N5	1.472 (5)	N5–C9	1.509 (5)
C9–C10	1.524 (5)	C9–C13	1.516 (5)
C10–C11	1.536 (6)	C11–N6	1.482 (5)
C11–C17	1.543 (6)	C11–C16	1.523 (6)
N6–C12	1.486 (5)	N6–O	1.288 (4)
C12–C13	1.534 (6)	C12–C14	1.532 (6)
C12–C15	1.538 (6)		
b. Bond Angles			
Cl1–Cu–Cl2	113.3 (1)	Cl1–Cu–N1	91.4 (1)
Cl1–Cu–N3	95.3 (1)	Cl1–Cu–N5	94.6 (1)
Cl2–Cu–N1	97.6 (1)	Cl2–Cu–N3	97.5 (1)
Cl2–Cu–N5	152.1 (1)	N1–Cu–N3	159.5 (1)
N1–Cu–N5	79.7 (1)	N3–Cu–N5	80.5 (1)
Cu–N1–N2	113.5 (2)	Cu–N1–C1	140.2 (3)
N2–N1–C1	106.1 (3)	N1–N2–C3	111.1 (3)
N1–N2–C7	120.0 (3)	C3–N2–C7	128.6 (3)
N1–C1–C2	110.4 (4)	C1–C2–C3	105.7 (4)
N2–C3–C2	106.7 (4)	Cu–N3–N4	112.3 (3)
Cu–N3–C4	141.4 (3)	N4–N3–C4	105.8 (4)
N3–N4–C6	110.7 (4)	N3–N4–C8	117.6 (3)
C6–N4–C8	131.7 (4)	N3–C4–C5	111.0 (5)
C4–C5–C6	105.7 (5)	N4–C6–C5	106.8 (4)
N2–C7–N5	108.2 (3)	N4–C8–N5	107.5 (3)
Cu–N5–C7	104.6 (2)	Cu–N5–C8	99.5 (2)
Cu–N5–C9	110.2 (2)	C7–N5–C8	112.4 (3)
C7–N5–C9	115.9 (3)	C8–N5–C9	112.6 (3)
N5–C9–C10	113.7 (3)	N5–C9–C13	111.5 (3)
C10–C9–C13	108.3 (3)	C9–C10–C11	113.4 (3)
C10–C11–N6	109.7 (3)	C10–C11–C17	111.6 (3)
N6–C11–C17	109.1 (3)	C10–C11–C16	108.9 (3)
N6–C11–C16	107.9 (3)	C17–C11–C16	109.5 (4)
C11–N6–C12	123.2 (3)	C11–N6–O	116.8 (3)
C12–N6–O	116.0 (3)	N6–C12–C13	109.9 (3)
N6–C12–C14	107.2 (3)	C13–C12–C14	107.8 (3)
N6–C12–C15	110.4 (3)	C13–C12–C15	111.8 (3)
C14–C12–C15	109.6 (4)	C9–C13–C12	113.9 (3)

<sup>a</sup>Estimated standard deviations in the least significant digits are given in parentheses.

Lorentz and polarization corrections were applied to the data.

The copper atom was located by inspection of peaks in the *E* map generated by the direct-methods routine SOLV. Subsequent Fourier difference electron density maps revealed all non-hydrogen ligand atoms. Neutral-atom scattering factors<sup>9</sup> and anomalous scattering contributions<sup>10</sup> were included for all atoms.

In the final model, all non-hydrogen atoms were given anisotropic thermal parameters. Hydrogen atoms were included in idealized positions (C–H = 0.96 Å, *U*(H) = 1.2[*U*<sub>iso</sub>(C)]). The refinement converged ((shift/esd)<sub>av</sub> < 0.012, (shift/esd)<sub>max</sub> = 0.084 over the last 10 cycles) to yield the residual indices shown in Table I. In the final difference electron density map, the highest peak (0.54 e Å<sup>-3</sup>) occurred near the copper atom. The minimum in the map was -0.64 e Å<sup>-3</sup>.

Final fractional atomic coordinates for all non-hydrogen atoms of Cu(bp-NO)Cl<sub>2</sub> may be found in Table II. Bond lengths and angles for Cu(bp-NO)Cl<sub>2</sub> are given in Table III. Anisotropic thermal parameters (Table S-I), calculated hydrogen atom coordinates (Table S-II), and structure factors (calculated and observed, ×10, Table S-III), have been included as supplementary material.

**Computer Simulations.** The simulations of the EPR spectra were obtained with CUNO<sup>11</sup> for fluid-solution data and with MENO<sup>12</sup> for fro-

(9) *International Tables for X-ray Crystallography*; Kynoch: Birmingham, England, 1974; Vol. IV, p 99.

(10) Reference 9, p 149.

(11) Eaton, S. S.; DuBois, D. L.; Eaton, G. R. *J. Magn. Reson.* **1978**, *32*, 251.

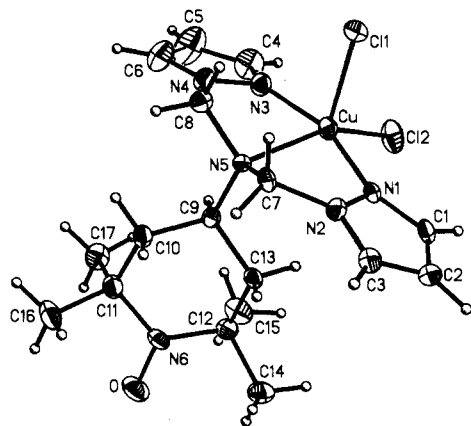


Figure 1. Thermal ellipsoid plot (50% probability) of  $\text{Cu}(\text{bp-NO})\text{Cl}_2$ . Hydrogen atoms have been included as spheres of fixed, arbitrary radius.

zen-solution data. The exchange term in the Hamiltonian was  $-JS_1S_2$ . The simulated fluid-solution spectra are not dependent on the sign of  $J$ .

### Results and Discussion

**$\text{Cu}(\text{bp-NO})\text{X}_2$  and  $\text{Cu}(\text{bdmp-NO})\text{X}_2$  ( $\text{X} = \text{Cl}, \text{Br}$ ).** The IR spectra of the complexes had a band at  $970\text{--}985\text{ cm}^{-1}$ . In the analogous complexes of  $\text{bdmp-ab}$  a band was reported at ca.  $975\text{ cm}^{-1}$  when the amine nitrogen atom was weakly coordinated.<sup>5</sup> The band shifted to ca.  $920\text{--}935\text{ cm}^{-1}$  when the amine nitrogen atom was not coordinated. Thus, the IR spectra of the  $\text{bdmp-NO}$  and  $\text{bp-NO}$  complexes suggested that the amine nitrogen atom was weakly coordinated. The visible spectra of  $\text{Cu}(\text{bdmp-NO})\text{X}_2$  ( $\text{X} = \text{Cl}, \text{Br}$ ) and  $\text{Cu}(\text{bp-NO})\text{X}_2$  ( $\text{X} = \text{Cl}, \text{Br}$ ) in fluid solution had broad d-d bands with maxima at about  $900\text{ nm}$  ( $11\,000\text{ cm}^{-1}$ ). Similar broad bands at  $9500\text{--}11\,500\text{ cm}^{-1}$  were reported for the solid reflectance spectra of  $\text{Cu}(\text{bdmp-R})\text{X}_2$  ( $\text{R} = \text{ae}, \text{ab}$ ;  $\text{X} = \text{Cl}, \text{Br}$ ).<sup>3,5</sup> Thus, the visible spectra suggested that the spin-labeled complexes were five-coordinate but also indicated that the visible spectra might not be a sensitive monitor of small changes in the geometry. Therefore, a crystal structure was obtained for  $\text{Cu}(\text{bp-NO})\text{Cl}_2$  to determine the detailed geometry around the  $\text{Cu}(\text{II})$  for comparison with the geometries of  $\text{Cu}(\text{bp-ae})\text{Br}_2$ <sup>4</sup> and  $\text{Cu}(\text{bdmp-ab})\text{Br}_2$ .<sup>5</sup>

**Structure of  $\text{Cu}(\text{bp-NO})\text{Cl}_2$ .** The structure of one of the discrete, five-coordinate, neutral complexes,  $\text{Cu}(\text{bp-NO})\text{Cl}_2$ , together with the numbering scheme used in the refinement, is displayed in Figure 1. The coordination geometry in this complex is best described as square pyramidal, with  $\text{Cl1}$  occupying the apical position. This assignment is supported by the long  $\text{Cu}\text{--}\text{Cl1}$  bond distance ( $2.495(1)\text{ \AA}$ , vs. a  $\text{Cu}\text{--}\text{Cl2}$  distance of  $2.231(1)\text{ \AA}$ ), which is expected for the bond to the apical atom in a square-pyramidal array around  $\text{Cu}(\text{II})$ , and by the angular parameter  $\tau$ ,<sup>13</sup> which is  $0.12$  for this complex ( $\tau = 0.0$  for idealized square-pyramidal geometry and  $1.0$  for idealized trigonal-bipyramidal geometry).

The structure for  $\text{Cu}(\text{bp-NO})\text{Cl}_2$  is very similar to that reported recently for  $\text{Cu}(\text{bp-ae})\text{Br}_2$  (angular parameter  $\tau = 0.12$ ).<sup>4</sup> The distances from the copper(II) ions to the two types of nitrogen atoms are nearly identical for the two structures, and even the difference ( $0.264\text{ \AA}$ ) between the two  $\text{Cu}\text{--}\text{Cl}$  distances in  $\text{Cu}(\text{bp-NO})\text{Cl}_2$  is nearly the same as the corresponding difference ( $0.288\text{ \AA}$ ) in the  $\text{Cu}\text{--}\text{Br}$  distances in  $\text{Cu}(\text{bp-ae})\text{Br}_2$ . The similarity in the  $\text{Cu}\text{--}\text{N}(\text{amine})$  distances in these two structures ( $\text{Cu}\text{--}\text{N5} = 2.195(3)\text{ \AA}$  in  $\text{Cu}(\text{bp-NO})\text{Cl}_2$ ,  $\text{Cu}\text{--}\text{N}(\text{amine}) = 2.191(2)\text{ \AA}$  in  $\text{Cu}(\text{bp-ae})\text{Br}_2$ ) is particularly striking, given the much shorter distances to tertiary, aliphatic amine atoms in other copper(II) complexes.<sup>14</sup> These similarities suggest that the coordinated

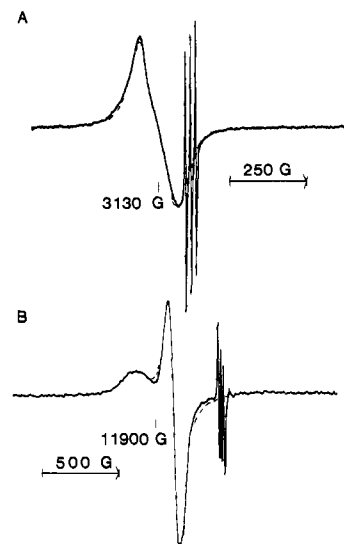


Figure 2. EPR spectra of  $\text{Cu}(\text{bp-NO})\text{Br}_2$  at room temperature: (A) 1000-G scan (X-band) of a solution in 1:2 toluene-dichloromethane obtained with 4-G modulation amplitude and 5-mW microwave power; (B) 2000-G scan (Q-band) of a toluene solution obtained with 12.5-G modulation amplitude and 5-mW microwave power. The dashed lines indicate regions in which the simulated spectra do not overlay the experimental data. The simulated spectra were obtained with  $J = 2000\text{ G}$ , copper and nitroxyl  $g$  values of 2.14 and 2.0059, respectively, and nuclear hyperfine splittings for copper and nitroxyl of 50 and 16 G, respectively.

halide,  $\text{Cl}^-$  or  $\text{Br}^-$ , does not have a large impact on the geometry of these complexes. However, these structures are strikingly different from the structure of  $\text{Cu}(\text{bdmp-ab})\text{Br}_2$ ,<sup>5</sup> in which the copper(II) ion has a distorted trigonal bipyramidal coordination environment (maximum  $\tau = 0.77$ ) and the  $\text{Cu}\text{--}\text{N}(\text{amine})$  distance is  $2.423(1)\text{ \AA}$ . Two factors may contribute to the differences in the structures. The steric effects of the 3,5-dimethylpyrazole substituents on the  $\text{bdmp-ab}$  ligand may favor the trigonal bipyramidal geometry. The lower basicity of the phenyl-substituted nitrogen atom in the  $\text{bdmp-ab}$  ligand than of the aliphatic-substituted nitrogen atoms in the  $\text{bp-ae}$  or  $\text{bp-NO}$  ligands may contribute to a lengthening of the  $\text{Cu}\text{--}\text{N}(\text{amine})$  bond that favors the trigonal bipyramidal geometry. In the  $\text{Co}(\text{bdmp-ab})\text{Cl}_2$  complex, the aniline nitrogen was not coordinated to  $\text{Co}(\text{II})$ , resulting in a four-coordinate, distorted tetrahedral complex,<sup>5</sup> while the  $\text{Ni}(\text{bdmp-ae})(\text{NO}_3)_2$  complex exhibited a distorted octahedral coordination sphere, in which the ethylamine nitrogen was coordinated.<sup>3</sup> These structures suggest that the basicity of the amine nitrogen is a significant factor in determining the strength of interaction between the metal ion and the amine nitrogen, although the differences between the metals and other changes in the coordination spheres may also contribute to differences in the binding of the amine nitrogen.

Other metric details of the structure of  $\text{Cu}(\text{bp-NO})\text{Cl}_2$  are unexceptional. The pyrazole rings are planar, as expected, with all deviations from the least-squares planes through the two rings less than  $0.01\text{ \AA}$ . The four basal coordinating atoms about copper(II) are an average of  $0.18\text{ \AA}$  from the least-squares plane through those atoms, while copper(II) is  $0.35\text{ \AA}$  above that plane. The copper(II) atom is only  $0.10\text{ \AA}$  above the plane through the three coordinating nitrogen atoms and is  $0.08\text{ \AA}$  from the plane of the pyrazole ring containing  $\text{N1}$  and  $0.19\text{ \AA}$  from the plane of the pyrazole ring containing  $\text{N2}$ .

**EPR Spectra of  $\text{Cu}(\text{bp-NO})\text{X}_2$  ( $\text{X} = \text{Cl}, \text{Br}$ ).** In dichloromethane solution the X-band spectra of  $\text{Cu}(\text{bp-NO})\text{Cl}_2$  and  $\text{Cu}(\text{bp-NO})\text{Br}_2$  had a signal at  $g = 2.07$  with partially resolved copper hyperfine splitting of about  $25\text{ G}$  (Figure 2A). A spectrum of  $\text{Cu}(\text{bdmp-ab})\text{Cl}_2$  in dichloromethane had  $g = 2.14$  and  $A_{\text{Cu}} = 48\text{ G}$ . The spectra of  $\text{Cu}(\text{bp-NO})\text{X}_2$  were therefore attributed

(12) Eaton, S. S.; More, K. M.; Sawant, B. M.; Boymel, P. M.; Eaton, G. R. *J. Magn. Reson.* **1983**, *52*, 435.

(13) Addison, A. W.; Rao, T. N.; Reedijk, J.; van Rijn, J.; Verschoor, G. C. *J. Chem. Soc., Dalton Trans.* **1984**, 1349.

(14) Karlin, K. D.; Hayes, J. C.; Juen, S.; Hutchinson, J. P.; Zubieta, J. *Inorg. Chem.* **1982**, *21*, 4106.

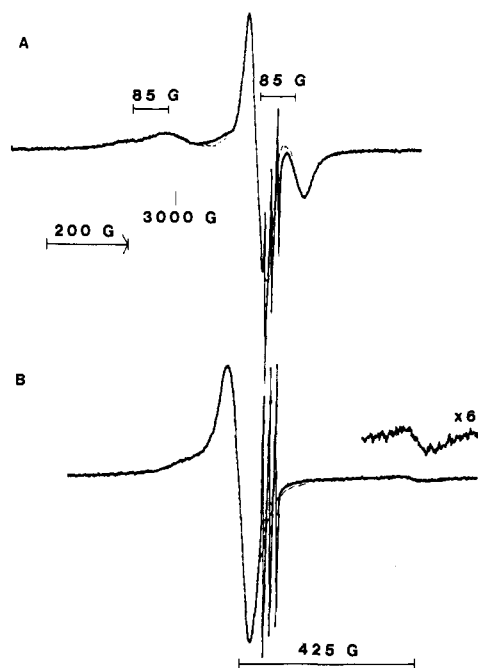


**Figure 3.** 1000-G scans of the X-band EPR spectra of  $\text{Cu}(\text{bdmp-NO})\text{X}_2$ : (A) spectrum in dichloromethane solution at 22 °C obtained with 5-mW microwave power and 2-G modulation amplitude; (B) spectrum in toluene solution at 10 °C obtained with 10-mW microwave power and 2-G modulation amplitude. The dashed lines indicate regions in which the simulated spectra do not overlay the experimental data. The simulated spectra were obtained with copper and nitroxyl  $g$  values of 2.13 and 2.0059, respectively, and nuclear hyperfine splittings for copper and nitroxyl of 50 and 16 G, respectively.

to exchange interaction between the copper and nitroxyl unpaired electrons that was sufficiently large relative to the  $g$ -value difference to give a signal at the average  $g$  value with half the value of  $A_{\text{Cu}}$  observed in the absence of spin-spin interaction.<sup>15,16</sup> The simulated spectrum was obtained with  $J = 2000$  G, although larger values of  $J$  gave comparable agreement with the experimental spectrum. The sharp three-line signal at  $g = 2.0$  was due to a small amount of nitroxyl that was not interacting with the copper(II) and was not included in the simulation.

A more accurate value of the electron-electron exchange coupling constant was obtained from the Q-band (35-GHz) spectrum of  $\text{Cu}(\text{bp-NO})\text{Br}_2$  in dichloromethane (Figure 2B). Separate signals were observed for the copper and nitroxyl "inner" lines of the AB splitting pattern. The "outer" lines were too weak to detect. At the higher frequency the  $g$ -value difference caused a larger separation between the copper and nitroxyl energy levels than that at X-band.<sup>17</sup> The value of  $J$  that gave one signal at the average of the copper and nitroxyl  $g$  values for  $\text{Cu}(\text{bp-NO})\text{Br}_2$  at X-band was not large enough to give an averaged signal at Q-band. The Q-band spectrum was simulated with  $J = 2000$  G which is consistent with the X-band data. The uncertainty in the value of  $J$  was about 200 G. When the temperature was decreased, the copper "inner" line broadened substantially due to incomplete motional averaging. The position of the nitroxyl "inner" line did not shift with temperature over the range  $-55$  to  $+22$  °C, which indicated that the value of  $J$  was not strongly temperature dependent.

The low solubility of  $\text{Cu}(\text{bp-NO})\text{X}_2$  limited the range of studies that could be performed in solution. The X-band spectrum of  $\text{Cu}(\text{bp-NO})\text{Br}_2$  in 1:1 toluene-dichloromethane was indistinguishable from that in dichloromethane. Thus, the limited data available do not indicate a strong dependence of the EPR spectra

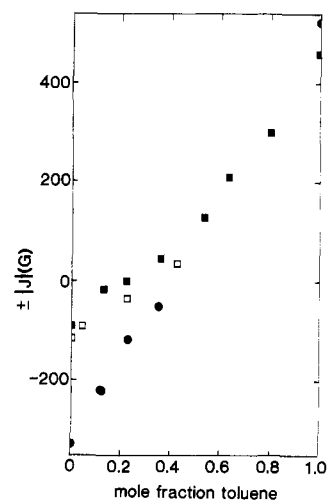


**Figure 4.** Plot of the electron-electron coupling constant,  $J$ , for  $\text{Cu}(\text{bdmp-NO})\text{X}_2$  ( $\text{X} = \text{Cl}, \text{Br}$ ) vs. the mole fraction of toluene in the solvent mixture: (■)  $\text{X} = \text{Cl}$ , second solvent dichloromethane; (●)  $\text{X} = \text{Br}$ , second solvent dichloromethane; (□)  $\text{X} = \text{Cl}$ , second solvent chloroform. The sign of  $J$  is not known so an arbitrary sign convention was used.

on solvent or temperature. Attempts to obtain spectra in frozen solution or on imbibitor beads<sup>18</sup> resulted in aggregation of the complexes.

**EPR Spectra of  $\text{Cu}(\text{bdmp-NO})\text{X}_2$  ( $\text{X} = \text{Cl}, \text{Br}$ ).** Two spectra that show the AB splitting patterns that typify the spectra of these complexes are shown in Figure 3. The value of  $J$  for the spectra in Figure 3 is 85 G. The splitting between the nitroxyl "inner" and "outer" lines is equal to  $J$  and is marked on the spectrum. The splitting of the copper lines is also equal to  $J$  but is less well-resolved due to the greater line widths of the copper lines than of the nitroxyl lines. For both pairs of signals the "inner" lines have greater intensity than the "outer" lines. The value of  $J$  for the spectrum in Figure 3B is 425 G. Comparison of the spectra in parts A and B of Figure 3 shows the characteristic changes that occur as the value of  $J$  increases—the "inner" lines move closer together and the intensity of the "outer" lines decreases. Due to the greater line width for the copper lines than for the nitroxyl lines, the copper "outer" lines were not observed in the spectrum shown in Figure 3B.

The values of  $J$  for  $\text{Cu}(\text{bdmp-NO})\text{X}_2$  ( $\text{X} = \text{Cl}, \text{Br}$ ) were strongly dependent on solvent. When the relative proportions of toluene and dichloromethane were varied, the absolute value of  $J$  passed through a minimum. The value of  $J$  for  $\text{Cu}(\text{bdmp-NO})\text{Cl}_2$  also passed through a minimum as the solvent composition was varied from chloroform to toluene. One interpretation of these results is that the value of  $J$  changed sign as the solvent was varied. A plot of  $J$  vs. the mole fraction of toluene is given in Figure 4, based on an arbitrary assumption concerning the signs of the values of  $J$ . The smooth variation in the values appears to support the proposal of a change of sign. The similarity in the values of  $J$  for  $\text{X} = \text{Cl}$  and  $\text{Br}$  (Figure 4) indicated that the bonding in the complexes was not strongly dependent on the anion.

In fluid solution the X-band EPR spectra of  $\text{Cu}(\text{bdmp-NO})\text{X}_2$  ( $\text{X} = \text{Cl}, \text{Br}$ ) were strongly dependent on temperature. The direction in which the magnitude of  $J$  changed with temperature depended on solvent. In toluene solution the magnitude of  $J$  decreased as the temperature was decreased. In chlorinated solvents and mixtures that were predominantly chlorinated solvents, the magnitude of  $J$  increased as the temperature decreased. The temperature dependence of the data is shown in Figure 5 with the same arbitrary sign convention as in Figure 4. The similarity in the slopes of the lines for all of the solvents suggests that there is a common temperature-dependent contribution to  $J$  and that contribution has the same sign as the net value of  $J$  in chlorinated solvents but is opposite to the sign of  $J$  in toluene.

(15) Eaton, S. S.; Eaton, G. R. *Coord. Chem. Rev.* **1978**, *26*, 207.

(16) Eaton, S. S.; More, K. M.; Sawant, B. M.; Eaton, G. R. *J. Am. Chem. Soc.* **1983**, *105*, 6560.

(17) Eaton, S. S.; More, K. M.; DuBois, D. L.; Boymel, P. M.; Eaton, G. R. *J. Magn. Reson.* **1980**, *41*, 150.

(18) More, K. M.; Eaton, G. R.; Eaton, S. S. *Anal. Chem.* **1984**, *56*, 1551.  
More, K. M.; Eaton, G. R.; Eaton, S. S. *J. Magn. Reson.* **1984**, *59*, 497.

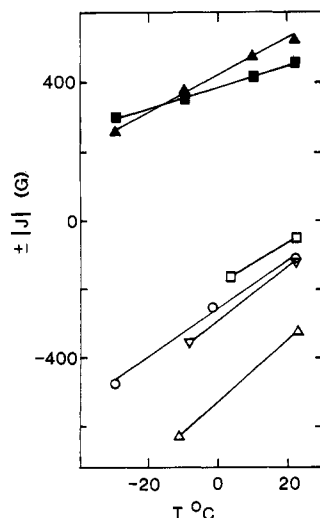


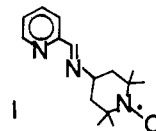
**Figure 5.** Plot of the temperature dependence of  $J$  for  $\text{Cu}(\text{bdmp-NO})\text{X}_2$  in various solvents with the same sign convention as in Figure 4: (■)  $\text{X} = \text{Cl}$  in toluene; (▲)  $\text{X} = \text{Br}$  in toluene; (□)  $\text{X} = \text{Cl}$  in 1:2 toluene-chloroform; (○)  $\text{X} = \text{Cl}$  in chloroform; (▽)  $\text{X} = \text{Br}$  1:1 toluene-dichloromethane; (△)  $\text{X} = \text{Br}$  in dichloromethane.

In frozen toluene-dichloromethane solution the EPR spectra of  $\text{Cu}(\text{bdmp-NO})\text{X}_2$  ( $\text{X} = \text{Cl}, \text{Br}$ ) were poorly resolved but indicated strong interaction between the copper and nitroxyl unpaired electrons, which is consistent with the rapid increase in  $J$  with decreasing temperature in fluid solution in chlorinated solvents. The relative intensity of the half-field transitions<sup>19</sup> for  $\text{X} = \text{Cl}$  and  $\text{Br}$  was  $2.7 \times 10^{-4}$ , which corresponds to a copper-nitroxyl distance of 6.5 Å. In the crystal structure of  $\text{Cu}(\text{bp-NO})\text{Cl}_2$  the through-space distances between the copper and the nitroxyl nitrogen and oxygen were 5.694 and 6.913 Å, respectively, for an average of 6.3 Å. The similarity between this average value and the copper-nitroxyl distance obtained from the EPR spectrum of  $\text{Cu}(\text{bdmp-NO})\text{Cl}_2$  suggests that the structure of  $\text{Cu}(\text{bdmp-NO})\text{Cl}_2$  in frozen solution does not differ greatly from the structure of  $\text{Cu}(\text{bp-NO})\text{Cl}_2$  observed in the crystal. It is therefore proposed that the increase in the value of  $J$  with decreasing temperature is due to a decrease in the length of the bond between the copper and the amine nitrogen.

**$\text{Cu}(\text{bdmp-NO})\text{X}_2$  ( $\text{X} = \text{ClO}_4, \text{BF}_4$ ).** In the IR spectra of these complexes there were strong peaks characteristic of the anion. The perchlorate band at  $1100 \text{ cm}^{-1}$  was split into several partially resolved peaks. The tetrafluoroborate peaks also were split ( $1040, 1080, 1120$  and  $520, 530 \text{ cm}^{-1}$ ). These splittings indicate coordination of the anions.<sup>20</sup> The visible spectra in dichloromethane solution had maxima at  $600\text{--}610 \text{ nm}$  (ca.  $16\,500 \text{ cm}^{-1}$ ), which is at substantially higher energy than was observed for five-coordinate  $\text{Cu}(\text{bdmp-R})\text{X}$  ( $\text{X} = \text{Cl}, \text{Br}$ ) ( $9500\text{--}11\,000 \text{ cm}^{-1}$ ) and somewhat higher than reported for six-coordinate  $\text{Cu}(\text{bdmp-Et})(\text{NO}_3)_2$  ( $13\,500 \text{ cm}^{-1}$ ).<sup>3</sup> The EPR spectrum of  $\text{Cu}(\text{bdmp-ab})(\text{ClO}_4)_2$  on imbibed beads had  $g = 2.05, 2.07, 2.24$  and  $A_{\parallel} = 172 \text{ G}$ . The observation of  $g_{\perp} < g_{\parallel}$  and the large value of  $A_{\parallel}$  suggest that these complexes are four- or six-coordinate rather than five-coordinate.<sup>21-24</sup> At both X-band and Q-band the EPR spectra of  $\text{Cu}(\text{bdmp-NO})\text{X}_2$  ( $\text{X} = \text{ClO}_4, \text{BF}_4$ ) in fluid solution had one signal

at the average of the copper and nitroxyl  $g$  values, which indicated strong exchange between the copper and nitroxyl unpaired electrons. To obtain an averaged signal at Q-band requires  $J > 3500 \text{ G}$  for this complex. There was no indication of solvent dependence of the spectra.

For comparison of the magnitude of  $J$ , EPR spectra were also obtained for  $\text{Cu}(\text{bdmp-ab})\text{Cl}_2$  bound to the spin-labeled ligand I. The amine nitrogen in this complex is expected to be strongly



bound to the copper. The EPR spectra showed strong exchange at both X-band and Q-band, which indicates  $J > 3500 \text{ G}$ .

**Comparison of the Values of  $J$  in Fluid Solution.** The largest values of  $J$  ( $> 3500 \text{ G}$ ) were observed for  $\text{Cu}(\text{bdmp-NO})\text{X}_2$  ( $\text{X} = \text{ClO}_4, \text{BF}_4$ ) and the complex of  $\text{Cu}(\text{bdmp-ab})\text{Cl}_2$  with the spin-labeled ligand I. In these complexes it is proposed that there is strong bonding between the copper and the nitrogen attached to the nitroxyl ring. Slightly smaller values of  $J$  (about  $2000 \text{ G}$ ) were observed for  $\text{Cu}(\text{bp-NO})\text{X}_2$  ( $\text{X} = \text{Cl}, \text{Br}$ ). The decrease in the value of  $J$  suggests a weaker bond between the copper and the amine nitrogen as observed in the crystal structure of  $\text{Cu}(\text{bp-NO})\text{Cl}_2$  (2.189 Å). These values of  $J$  were not strongly dependent on solvent or temperature. Much smaller values of  $J$  were observed for  $\text{Cu}(\text{bdmp-NO})\text{X}_2$  ( $\text{X} = \text{Cl}, \text{Br}$ ). It is proposed that this was due to a much weaker bond between the copper and the amine nitrogen, similar to what was observed in  $\text{Cu}(\text{bdmp-ab})\text{Br}_2$  (2.423 Å). These values of  $J$  were strongly dependent on temperature, which suggests that the weak spin-spin interactions were sensitive to small changes in geometry. The weaker Cu-N(amine) bond in  $\text{Cu}(\text{bdmp-NO})\text{X}_2$  than in  $\text{Cu}(\text{bp-NO})\text{X}_2$  suggests that the steric effect of the 3,5-dimethylpyrazole substituents has a significant effect on the geometry of the complexes.

There are two potential pathways for the copper-nitroxyl exchange interaction in these complexes. When there is a bond between the copper and the amine nitrogen, exchange interaction can occur through that bond. The relative importance of ferromagnetic and antiferromagnetic contributions may depend on bond length and may vary as the geometry shifts from distorted square pyramidal to distorted trigonal bipyramidal. Interaction can also occur via the bond of the copper to the pyrazole nitrogens and through the intervening bonds to the nitroxyl ring. The presence of a  $\text{CH}_2$  group in the latter pathway is expected to limit the value of  $J$  to a significantly smaller value than could be obtained by a strong interaction of the copper with the amine nitrogen. If the interaction of the copper with the amine nitrogen is weak, the contribution to the copper-nitroxyl interaction from the bond to the pyrazole nitrogen may be comparable in magnitude to the interaction via the amine nitrogen. If the two contributions are of opposite sign, changes in the magnitudes of the two terms could result in a change in the sign of  $J$ .

**Acknowledgment.** This work was supported in part by NIH Grant GM21156 (G.R.E. and S.S.E.). Purchase of the IBM ER200 EPR spectrometer was funded in part by NSF Grant CHE8411282. The Nicolet R3m/E X-ray diffractometer and computing system at Colorado State University was purchased with funds provided by the National Science Foundation (Grant CHE81-03011). FAB mass spectra were obtained at the Mass Spectrometry Research Resource at the University of Colorado Health Science Center, which receives partial support from the NIH Division of Research Resources, Grant RR01152.

**Supplementary Material Available:** Anisotropic thermal parameters (Table S-I) and calculated hydrogen atom coordinates (Table S-II) (4 pages); structure factors (Table S-III) (20 pages). Ordering information is given on any current masthead page.

- (19) Eaton, S. S.; More, K. M.; Sawant, B. M.; Eaton, G. R. *J. Am. Chem. Soc.* **1983**, *105*, 6560.  
 (20) Foley, J.; Kennefick, D.; Phelan, D.; Tyagi, S.; Hathaway, B. *J. Chem. Soc., Dalton Trans.* **1983**, 2333.  
 (21) Hathaway, B. J.; Billing, D. E. *Coord. Chem. Rev.* **1970**, *5*, 143.  
 (22) Bencini, A.; Bertini, I.; Gatteschi, D.; Scozzafava, A. *Inorg. Chem.* **1978**, *17*, 3194.  
 (23) Reinen, D. *Comments Inorg. Chem.* **1983**, *2*, 227.  
 (24) Bencini, A.; Gatteschi, D. *Transition Met. Chem. (N.Y.)* **1982**, *8*, 1.